STATISTICAL PROPERTIES OF THE LARGE SCALE STRUCTURES:

21cm COSMOLOGY

For a review: https://iopscience.iop.org/article/10.1088/1742-6596/956/1/012003/pdf
https://arxiv.org/pdf/2203.17039

21-CM RADIATION

21-cm radiation originates from the hyperfine transition (spin-flip) of the hydrogen atom:

- **Strongly forbidden line, $t_{1/2}$ ~10^7 yr**
- **HI very abundant**
- **Spectrally isolated**
- **Small obscuration**
- **Earth's atmosphere is transparent to radio frequencies**

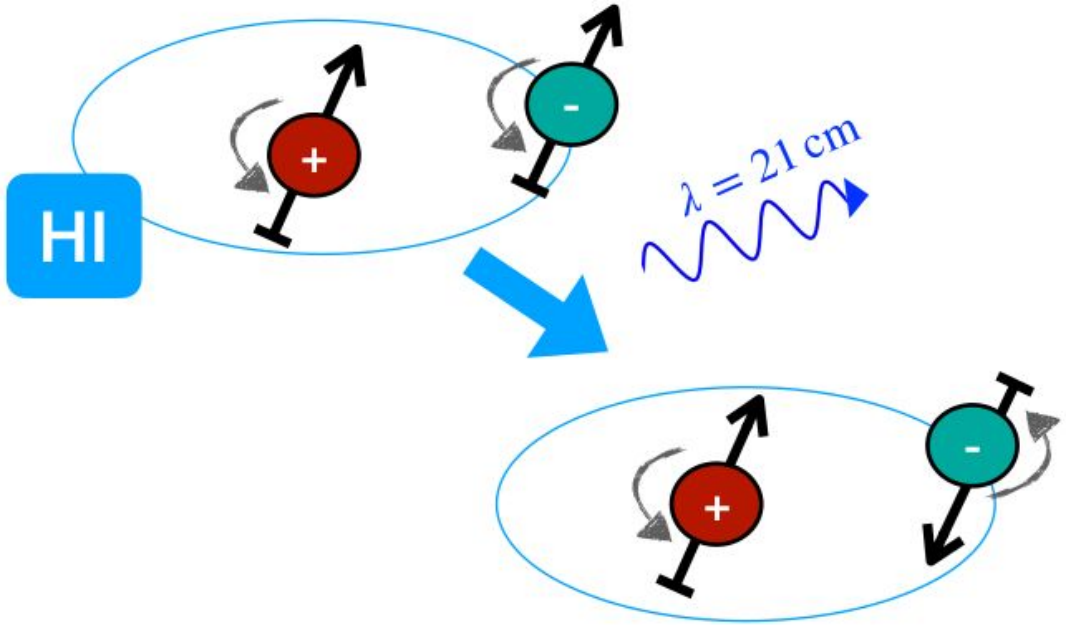

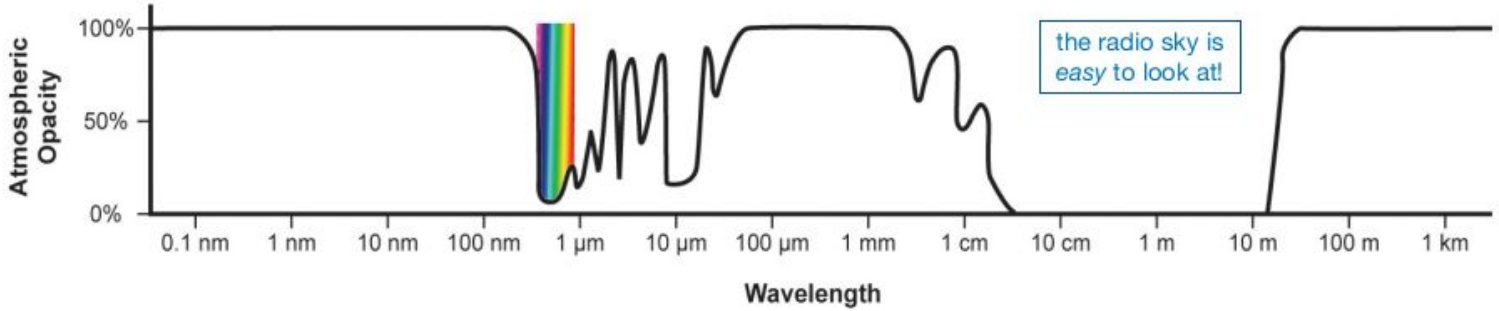

21-CM RADIATION FROM NEARBY GALAXIES

Assuming that the hydrogen atoms are uniformly distributed throughout galaxies, each line of sight through the galaxy will reveal a hydrogen line. The only difference between each of these lines is the Doppler shift that each of these lines has.

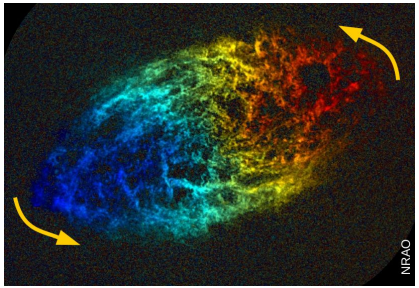

Observations of the hydrogen line have been used to reveal the spiral shape of the Milky Way and to calculate the mass and dynamics of individual galaxies through their velocity rotation curve.

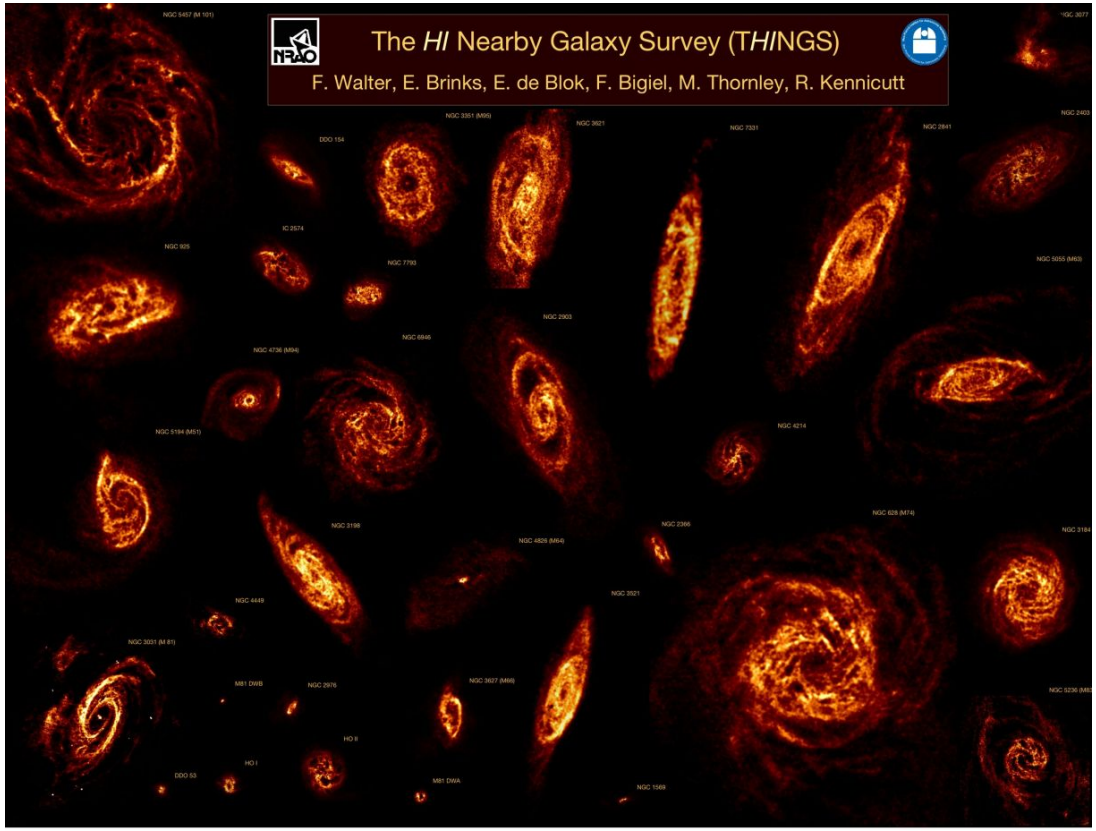

21-CM INTENSITY MAPPING

Intensity mapping is an observational technique for surveying the large-scale structure of the universe by using the integrated radio emission from unresolved HI gas clouds.

The frequency of the emission line is redshifted by the expansion of the Universe, thus the signal can be used to reconstruct the matter density field over cosmic time (tomography).

Intensity mapping surveys can be carried out much faster than conventional optical redshift surveys; it is possible to map-out significantly larger volumes of the Universe.

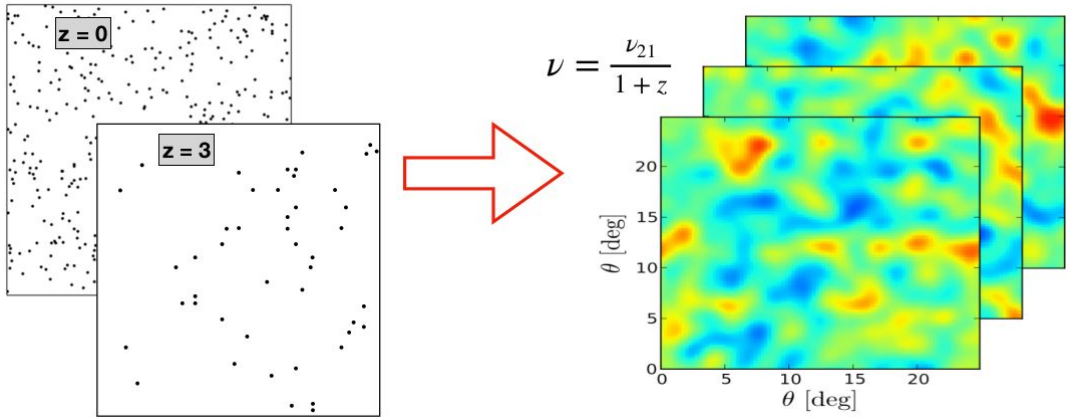

21-CM INTENSITY MAPPING

It can be used to probe the cosmological "dark ages" from recombination (when stable hydrogen atoms first formed) to reionization:

- **It can provide a picture of how the universe was re-ionized: neutral hydrogen which has been ionized by radiation from stars or quasars will appear as holes in the 21 cm background.**

- **By mapping the intensity of redshifted 21 cm radiation – λ = 21cm×(1+z) – it can measure the matter power spectrum in the period after recombination (BAO, RSD, etc, etc).**

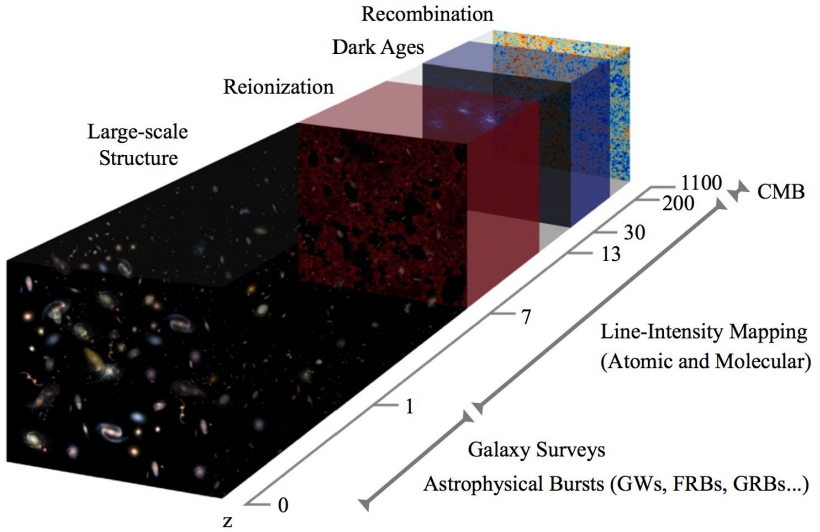

1. Large areas

2. Deep and accurate redshifts (distances)

3. Better coverage of the Universe epochs

21-CM INTENSITY MAPPING POWER SPECTRUM

- **Cosmic HI density** - $\Omega_{HI} \propto \bar{T}_{HI}$ overall amplitude of the power spectrum
- **HI bias** - amplitude plus non-linear scale-dependence
- **HI shot noise** - Poisson noise on the power spectrum depending on number densities
- $P_{HI}(k) = \bar{T}_{HI} b_{HI} P_{DM} + \mathrm{SN}$

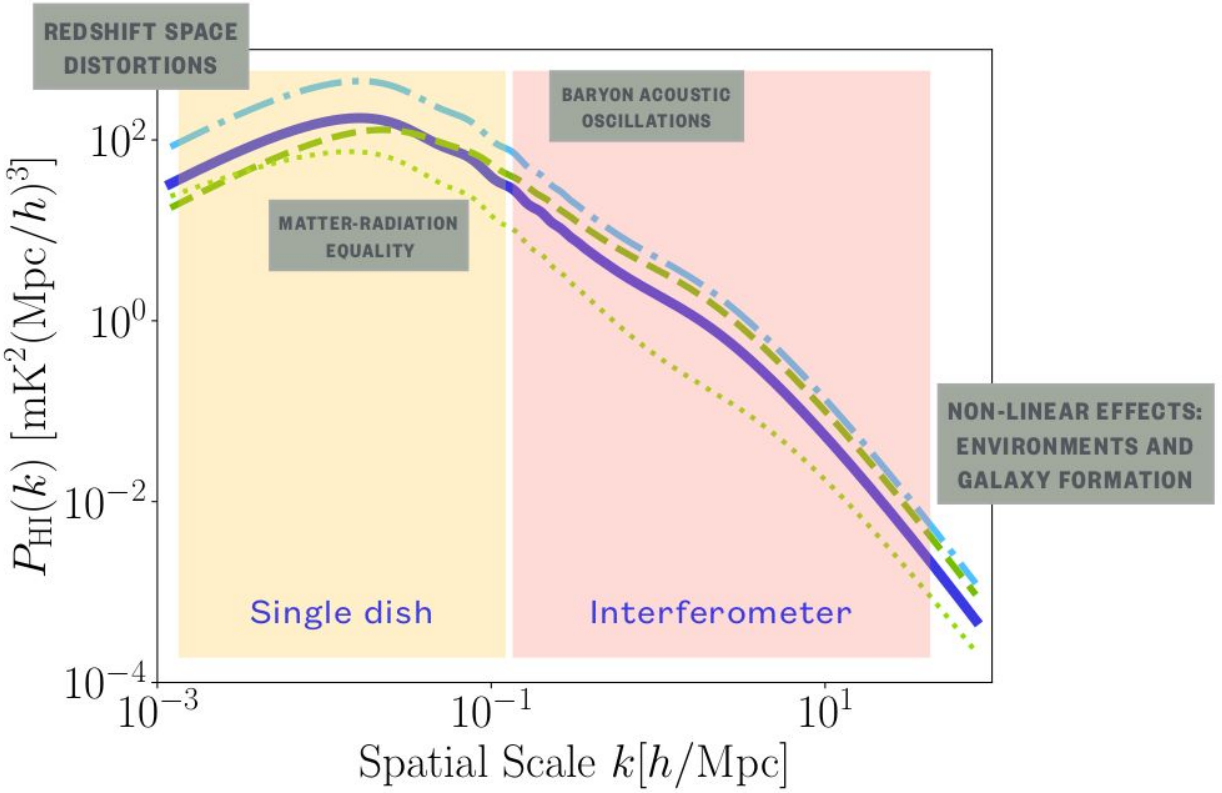

21-CM INTENSITY MAPPING

SKAO

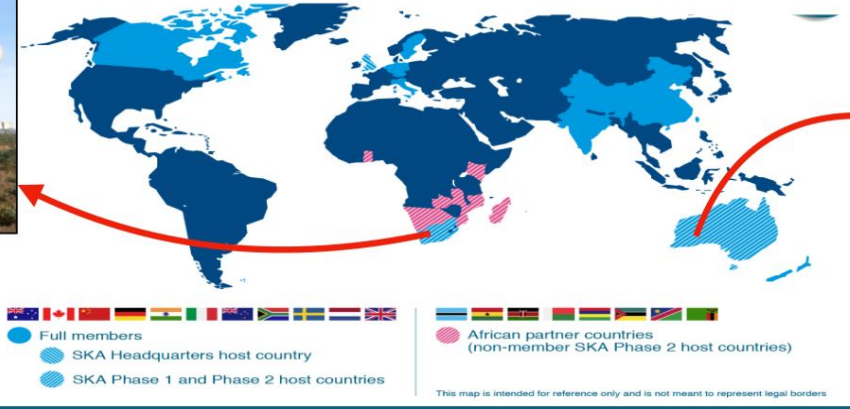

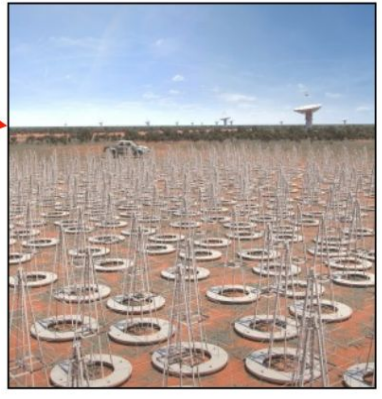

SKA1-mid
the SKA's mid-frequency instrument

0 < z < 3

Location: South Africa

Frequency range:
350 MHz to **15.3 GHz**
with a goal of 24 GHz

197 dishes
(including 64 MeerKAT dishes)

Maximum baseline:
150km

SKA1-low
the SKA's low-frequency instrument

3 < z < 27

Location: Australia

Frequency range:
50 MHz to **350 MHz**

~131,000
antennas spread between
512 stations

Maximum baseline:
~65km

21-CM INTENSITY MAPPING

Wide Survey of 20,000 deg² at 0.35-1.05 GHz for
- Continuum galaxy survey with ~100 million objects
- HI intensity maps for 0.35<z<3

Deep Survey 100 deg² at 200-350 MHz for
- HI intensity maps for 3<z<6

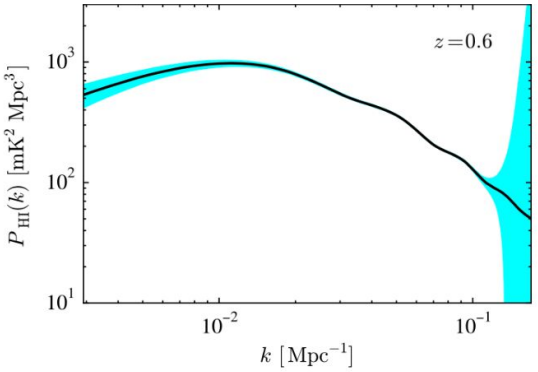

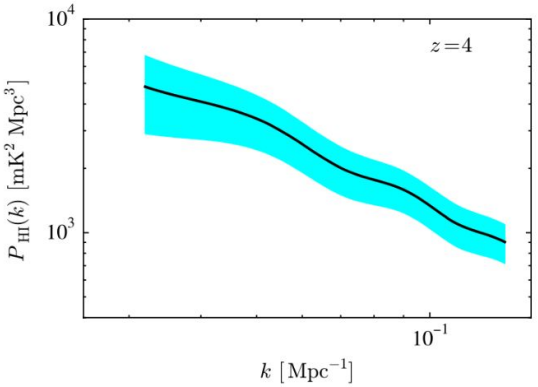

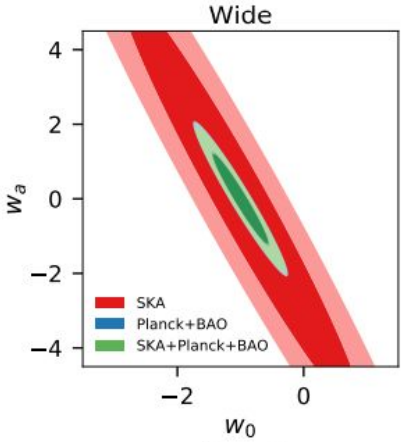

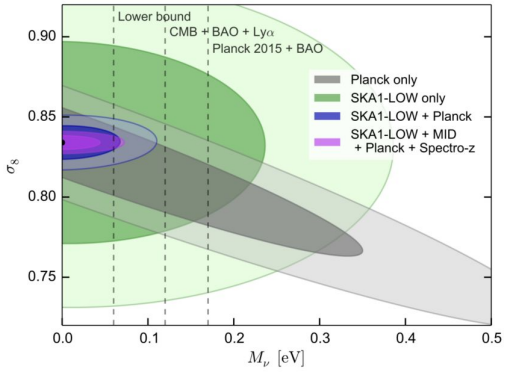

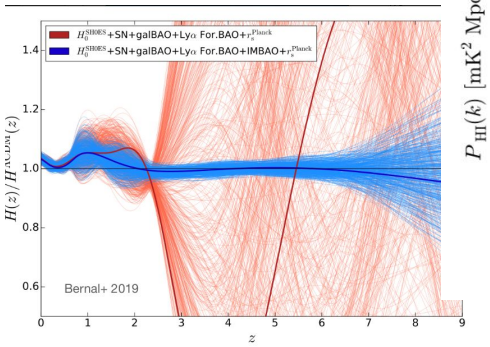

https://arxiv.org/abs/1811.02743

21-CM INTENSITY MAPPING

CHALLENGES:
The IM signal is weak compared to the contaminants

- **Receiver Noise: amplitude comparable to signal -> isotropic, 1/f noise can be removed, manageable in power spectrum space**
- **Instrumental errors: calibration uncertainties, sidelobes, pointing errors, polarization leakage**
- **Radio Frequency Interference: contaminates in spatial and frequency space -> go to the desert, stay away from satellites**
- **Foreground contaminations: Galactic emission and extra-Galactic point sources**

SIGNAL INTENSITY

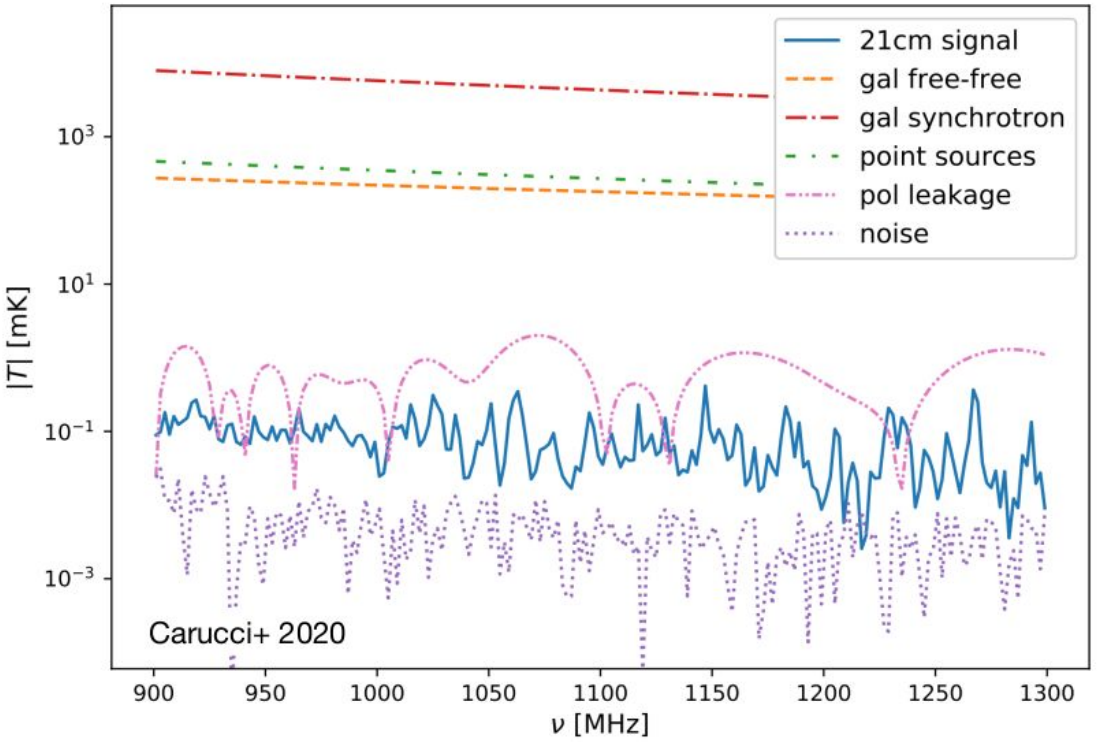

COSMOLOGY WITH GRAVITATIONAL WAVES

For a review: http://arXiv.org/abs/0903.0338v1

https://wwwmpa.mpa-garching.mpg.de/~komatsu/lecturenotes/Azadeh_Maleknejad_on_GW.pdf

https://onlinelibrary.wiley.com/doi/10.1002/andp.202200180

MULTI-MESSENGER COSMOLOGY

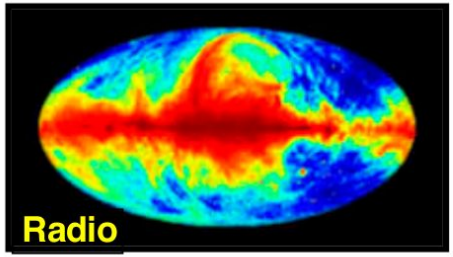

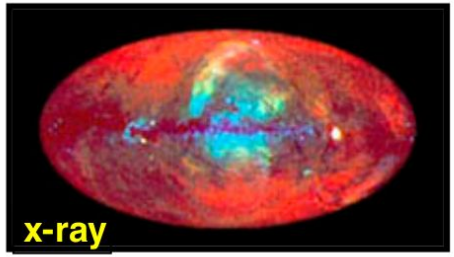

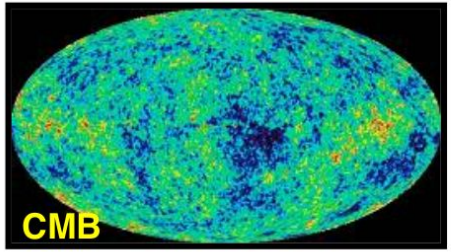

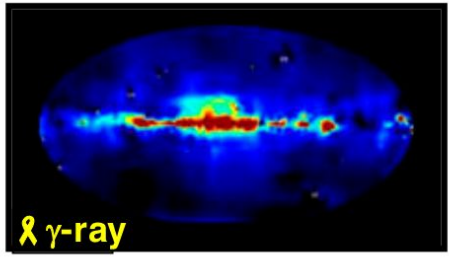

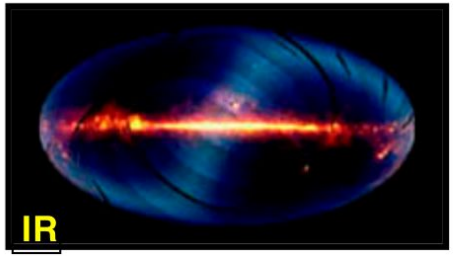

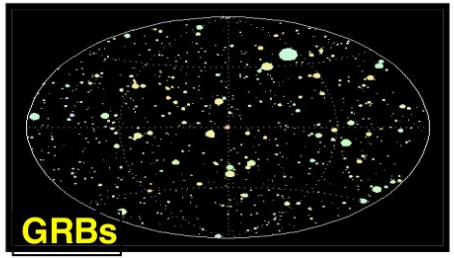

Most of what we know about the Universe is through photons.

Lot of ongoing efforts to obtain information about the universe using non-EM cosmic messengers.

MULTI-MESSENGER COSMOLOGY: COSMIC NEUTRINOS

First detection from Supernova 1987 by IMB , Kamioka (2002 Nobel prize M. Koshiba)

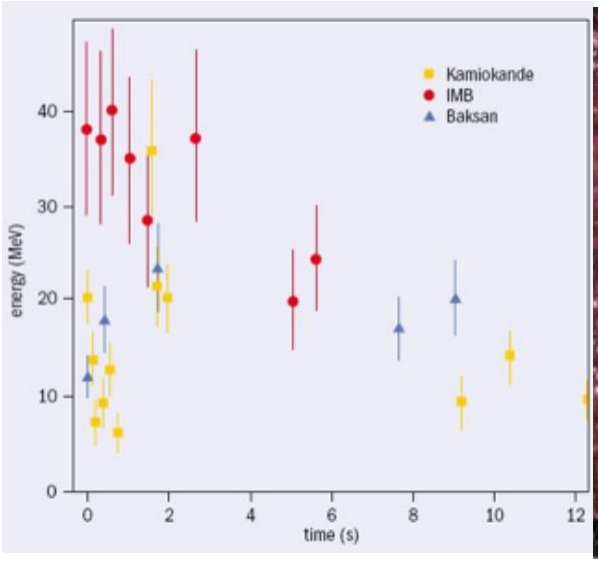

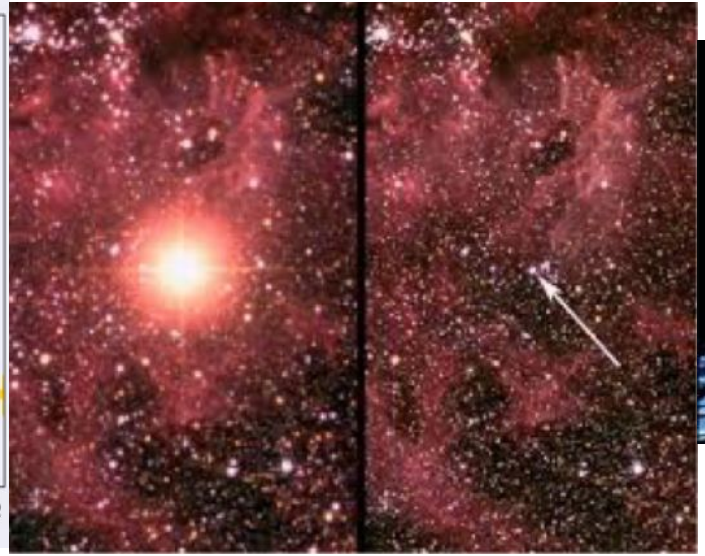

IMB detector

MULTI-MESSENGER COSMOLOGY: COSMIC NEUTRINOS

The IceCube Neutrino Observatory, located at the South Pole, is designed to detect highenergy (≳1 TeV) astrophysical neutrinos and identify their sources. The detector construction, which deployed instruments within a cubic kilometer of clear ice, was completed in 2011; 5160 digital optical modules (DOMs) were placed at depths between 1.5 and 2.5 km below the surface of the Antarctic glacial ice sheet. Neutrinos are detected through Cherenkov radiation, emitted by charged secondary particles that are produced by neutrino interactions with nuclei in the ice or bedrock. Because of the large momentum transfer from the incoming neutrino, the directions of secondary particles are closely aligned with the incoming neutrino direction, enabling the identification of the neutrino's origin.

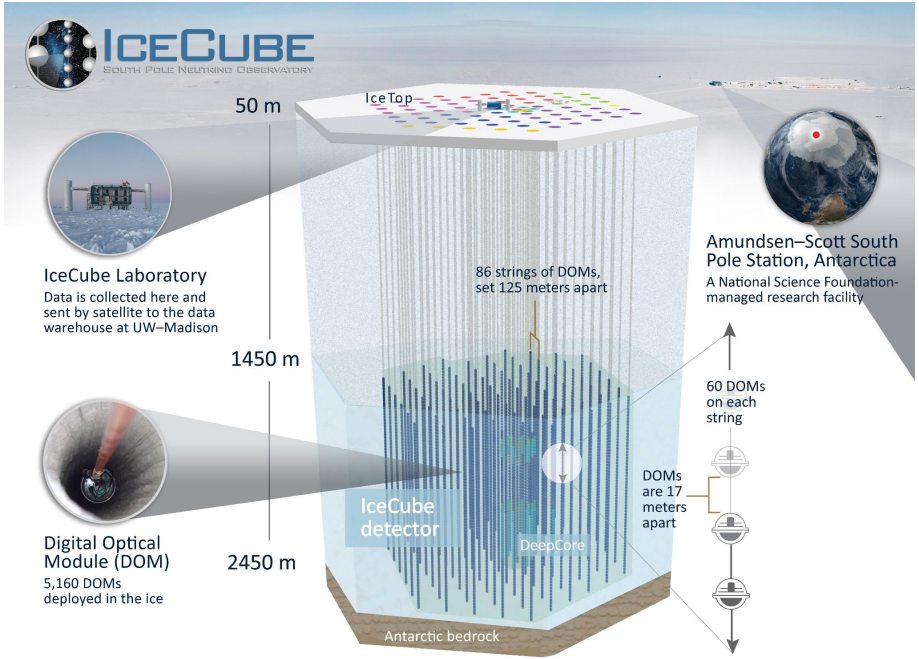

MULTI-MESSENGER COSMOLOGY: COSMIC NEUTRINOS

High-energy neutrinos from the MW Galactic plane seen by IceCube Neutrino Observatory

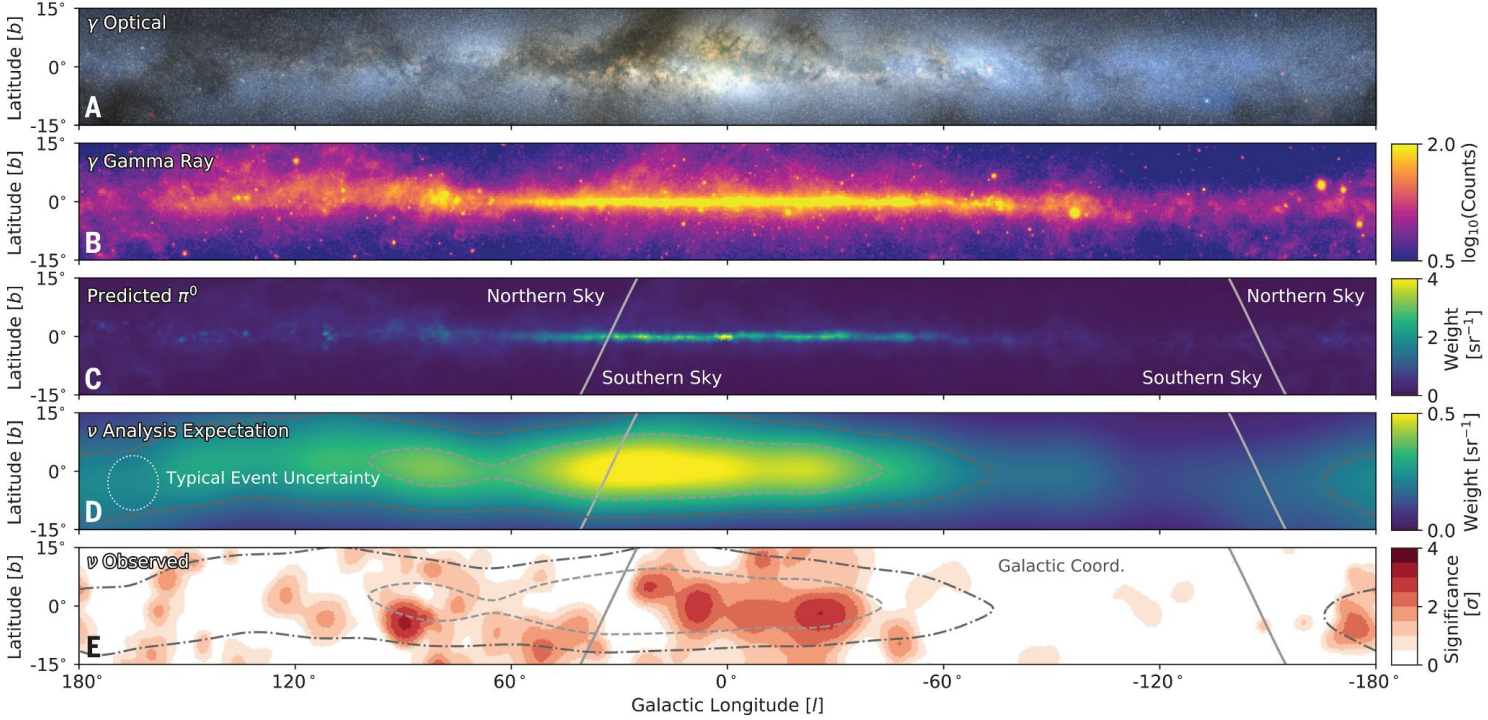

(A) to (E) are in Galactic coordinates, with the origin being at the Galactic Center, extending ±15° in latitude and ±180° in longitude. (**A**) Optical color image (*39*), which is partly obscured by clouds of gas and dust that absorb optical photons. [Credit: A. Mellinger, used with permission.] (**B**) The integrated flux in gamma rays from the Fermi Large Area Telescope (Fermi-LAT) 12-year survey (*40*) at energies greater than 1 GeV, obtained from the Fermi Science Support Center and processed with the Fermi-LAT ScienceTools. (**C**) The emission template calculated for the expected neutrino flux, derived from the π_0 template that matches the Fermi-LAT observations of the diffuse gamma-ray emission (*1*). (**D**) The emission template from (C), after including the detector sensitivity to cascade-like neutrino events and the angular uncertainty of a typical signal event (7°, indicated by the dotted white circle). Contours indicate the central regions that contain 20 and 50% of the predicted diffuse neutrino emission signal. (**E**) The pretrial significance of the IceCube neutrino observations, calculated from the all-sky scan for point-like sources by using the cascade neutrino event sample. Contours are the same as in (D). Gray lines in (C) to (E) indicate the northern-southern sky horizon at the IceCube detector.

https://www.science.org/doi/10.1126/science.adc9818

MULTI-MESSENGER COSMOLOGY: COSMIC NEUTRINOS

Extragalactic High-energy neutrinos seen by IceCube Neutrino Observatory

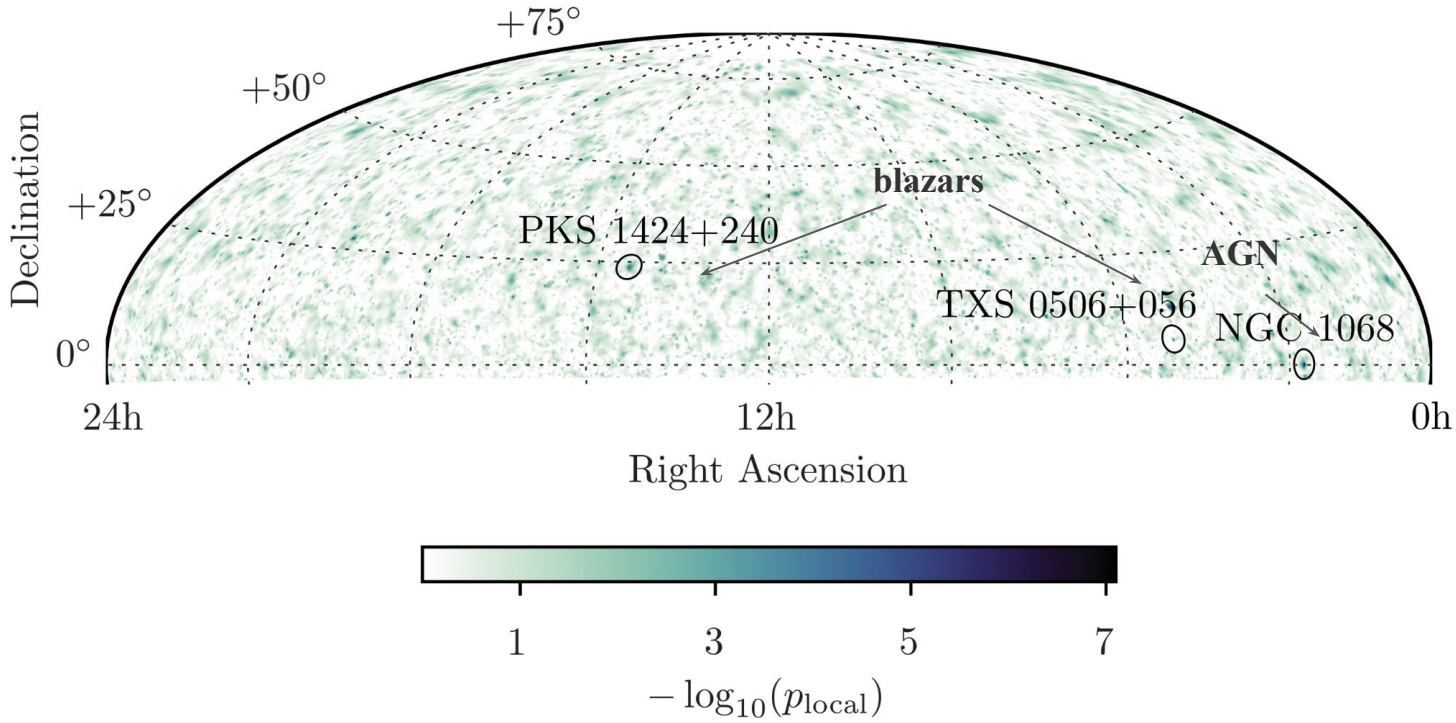

https://www.science.org/doi/10.1126/science.abg3395

GRAVITATIONAL WAVES

General Relativity predicts that space-time perturbations propagate through empty space at the speed of light.

$$\left(-\frac{\partial^2}{\partial t^2}+\nabla^2\right)\bar{h}^{\alpha\beta}=0.$$

Two possible polarizations:

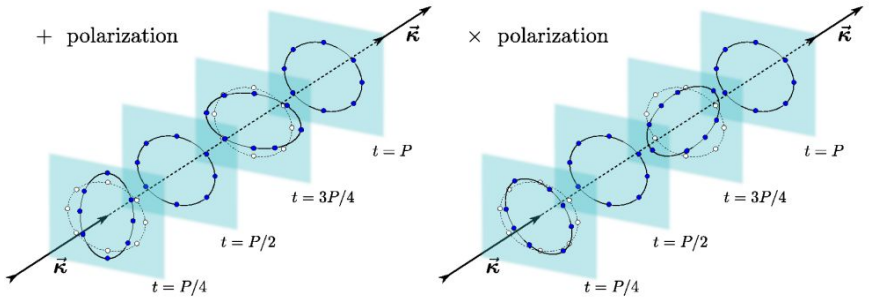

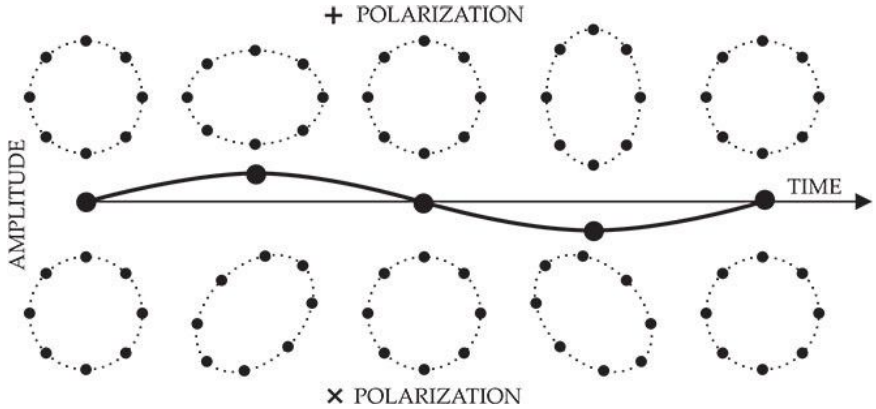

GRAVITATIONAL WAVES

PSR B1913+16: First indirect evidence from orbital period decay of binary system composed of a neutron star and pulsar, a rapidly rotating, highly magnetized neutron star (1993 Nobel prize J. Taylor, R. Hulse): the orbital decay match the energy loss predicted from GR due to gravitational wave radiation.

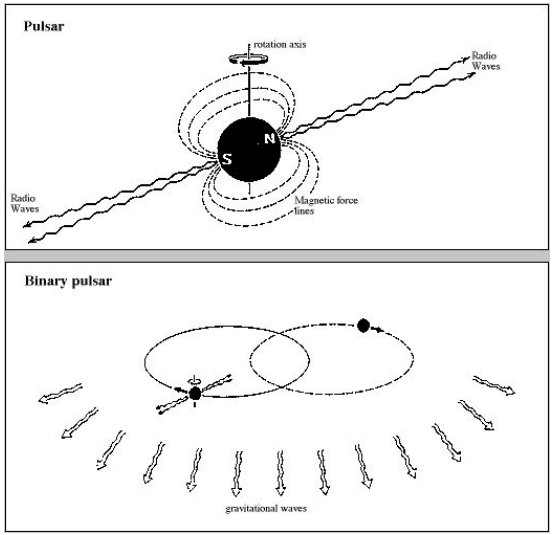

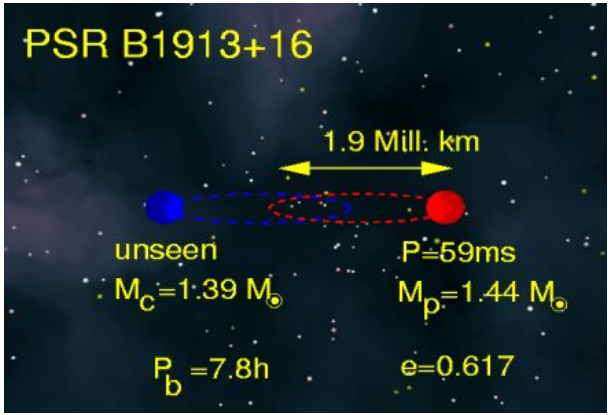

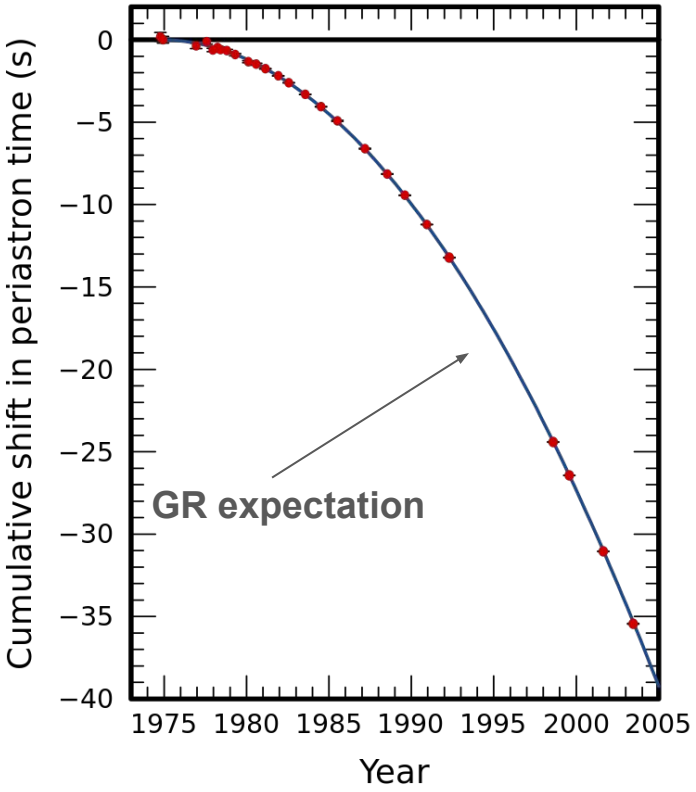

GRAVITATIONAL WAVE SPECTRUM

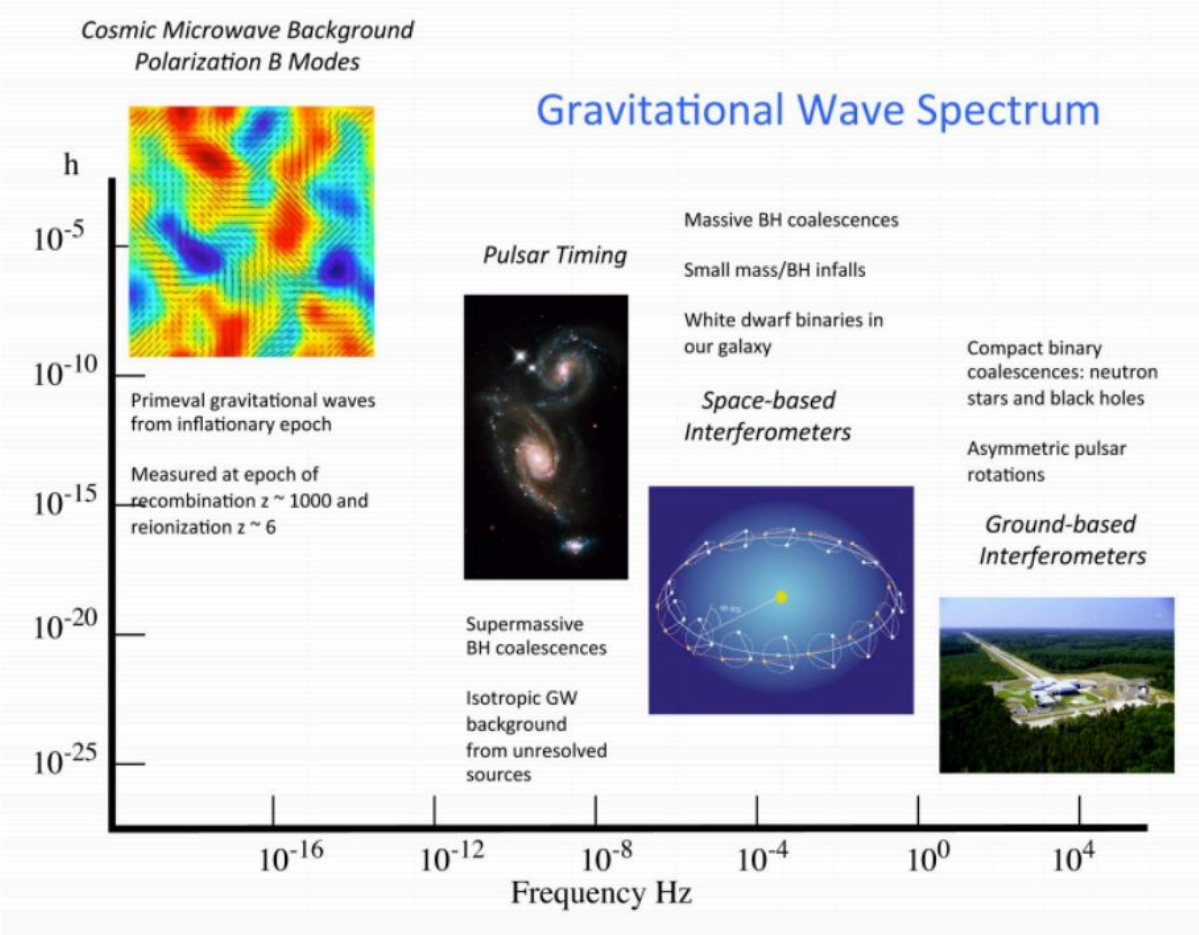

GRAVITATIONAL WAVE INTERFEROMETERS

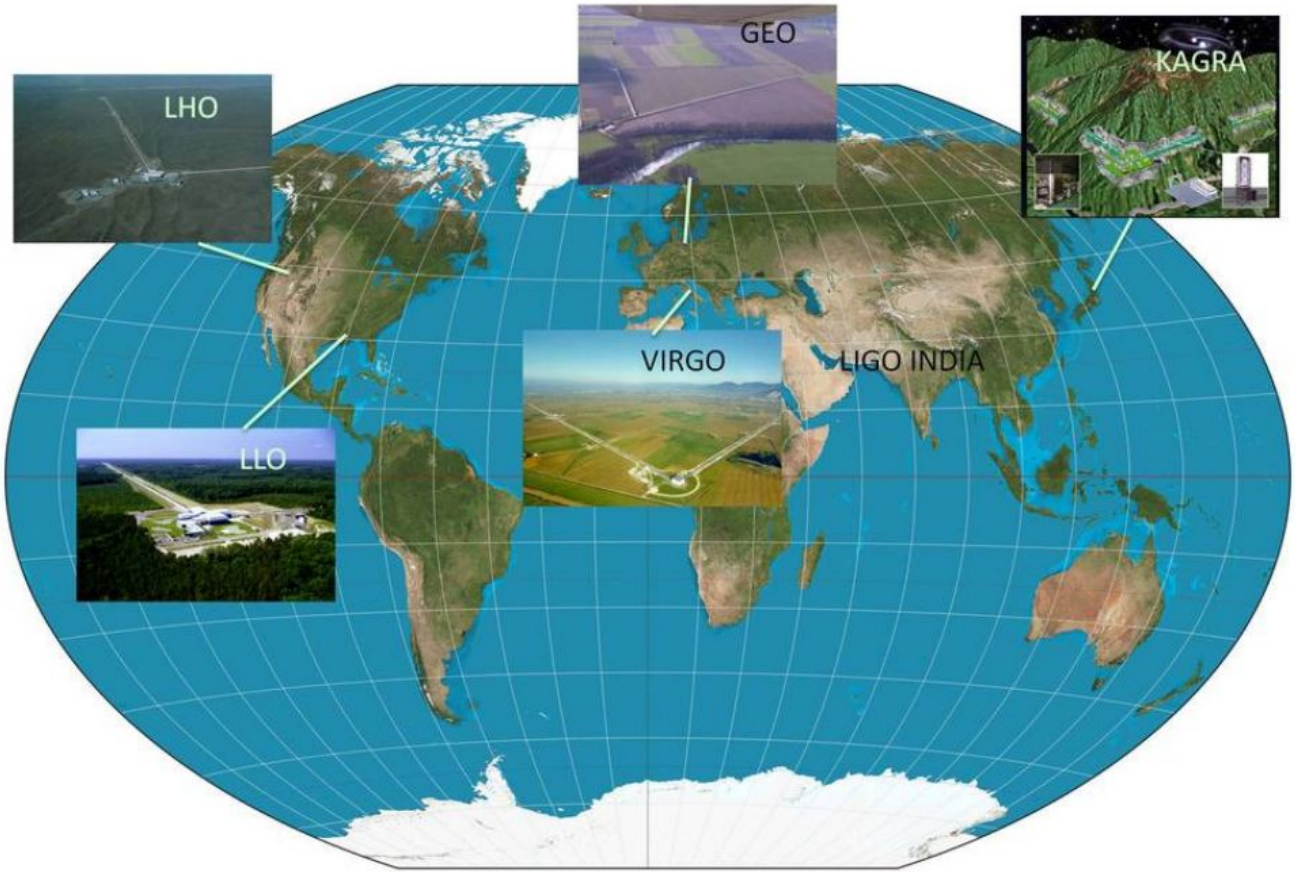

GRAVITATIONAL WAVE INTERFEROMETERS

LIGO & VIRGO Detectors

LIGO observatory contains 2 (H2) km and 4 km (H1) interferometers at Hanford, WA and a 4 km interferometer at Livingston, LA (L1) separated by 3000 km (10ms)

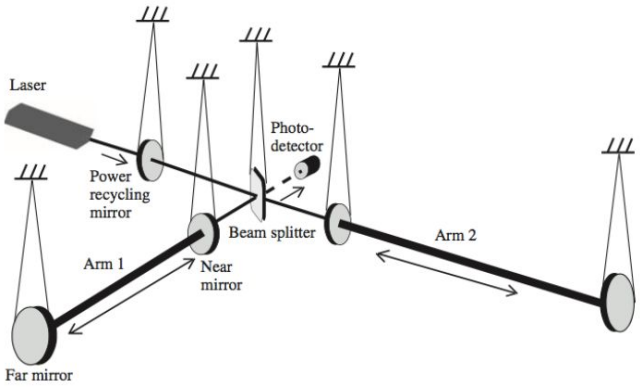

GRAVITATIONAL WAVE INTERFEROMETERS

For a binary system the wave's frequency sweep and amplitude depend on $\mathscr{M} = (m_1 m_2)^{3/5}/(m_1 + m_2)^{1/5}$, and luminosity distance:

$$\frac{d\Omega}{dt} \propto \left(\frac{G\mathcal{M}}{c^3}\right)^{5/3}$$

$$h \propto \frac{1}{D_L}\left(\frac{G\mathcal{M}}{c^3}\right)^{5/3}\Omega^{2/3}$$

Dimensionless strain, $h = \Delta l/l$, is the main observable measured; the typical relative deformation:

$$h = \frac{\Delta l}{l} \sim 10^{-21}$$

E.g. for the Laser Interferometer Gravitational-Wave Observatory (LIGO):

$l \sim 4\text{km} \rightarrow \Delta l \sim 10^{-16}\text{cm}$

GRAVITATIONAL WAVE INTERFEROMETERS

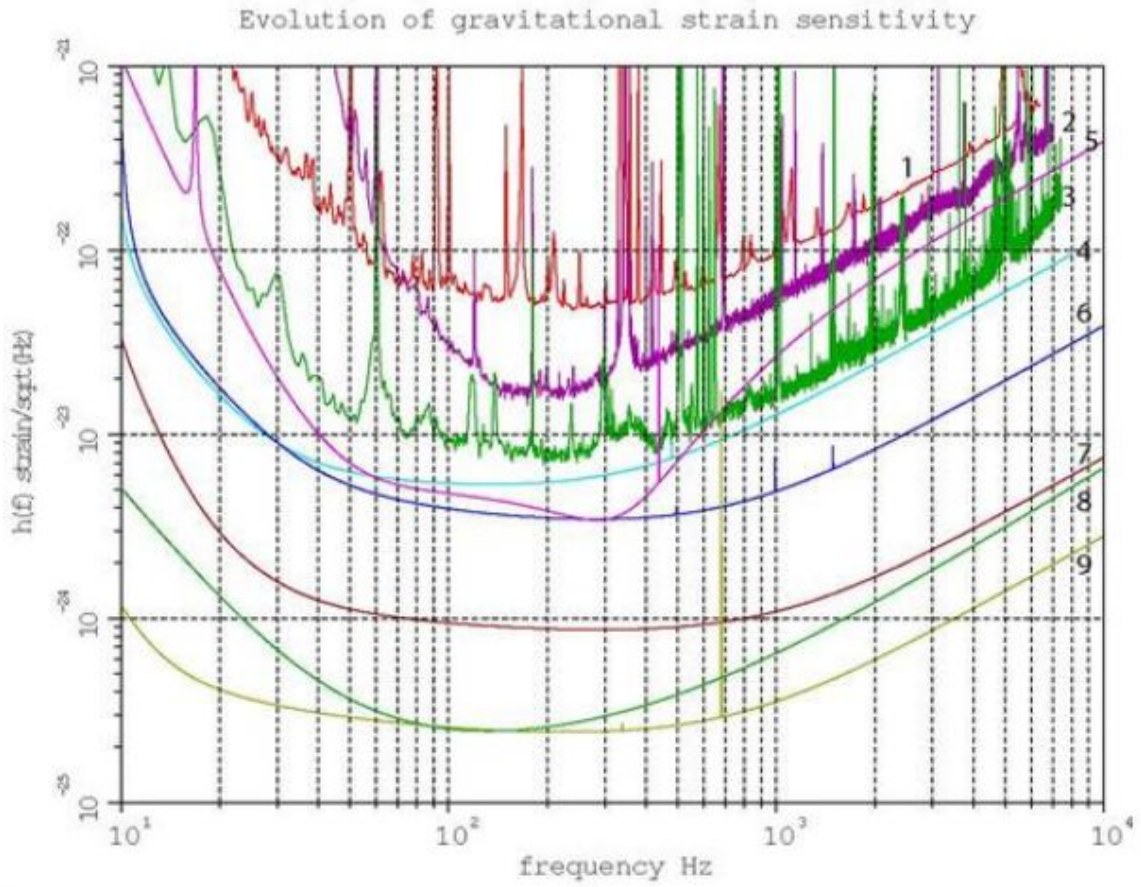

1 VIRGO 2009
2 Enhanced LIGO 2009
3 Advanced LIGO 65Mpc NS/NS 2015
4 Advanced LIGO 150Mpc NS/NS Low Power
5 Advanced VIRGO
6 Advanced LIGO 190Mpc NS/NS High Power
7 4km "Voyager" example 600Mpc NS/NS
8 Einstein telescope B
9 40km "Cosmic Explorer" example

GRAVITATIONAL WAVE INTERFEROMETERS

GW150914: First LIGO detection

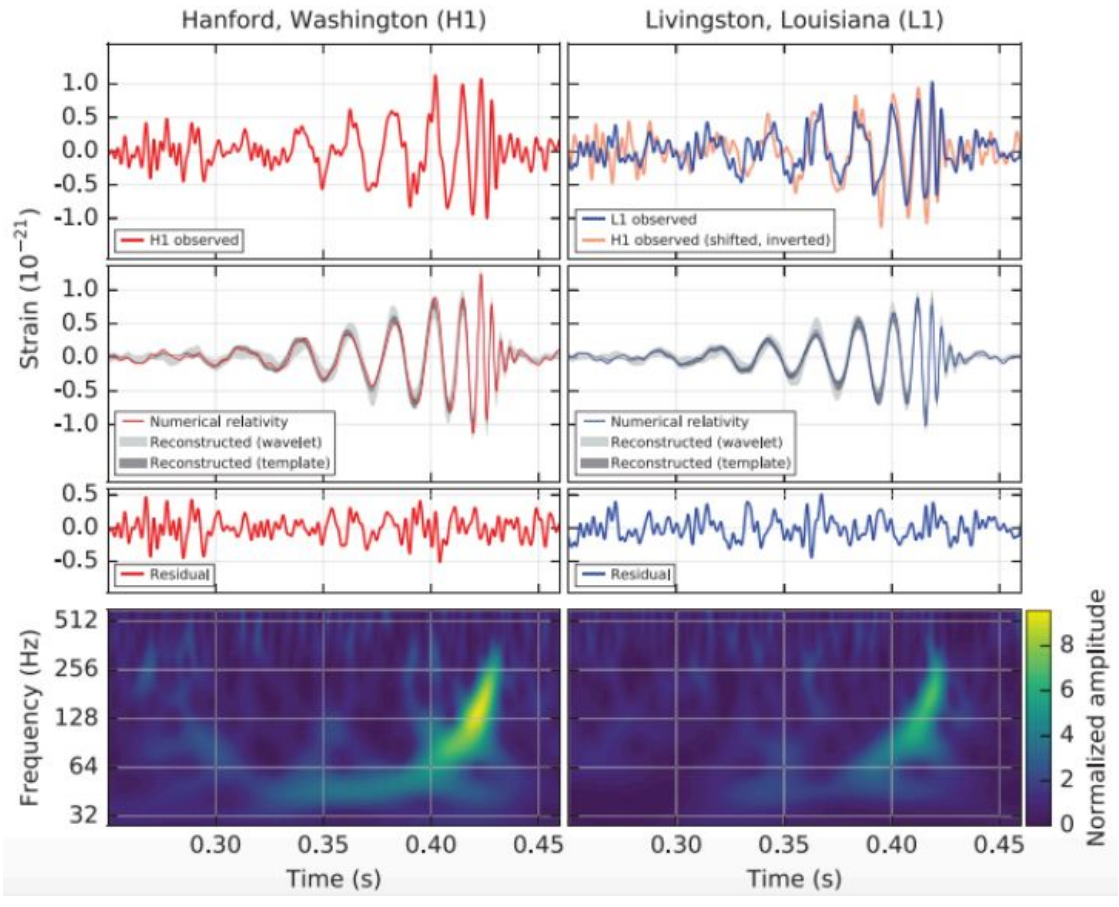

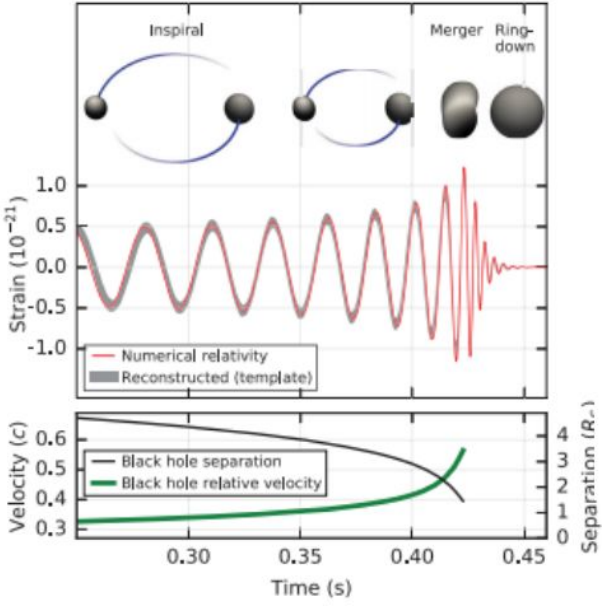

Primary black hole mass	$36^{+5}_{-4} M_\odot$
Secondary black hole mass	$29^{+4}_{-4} M_\odot$
Final black hole mass	$62^{+4}_{-4} M_\odot$
Final black hole spin	$0.67^{+0.05}_{-0.07}$
Luminosity distance	410^{+160}_{-180} Mpc
Source redshift z	$0.09^{+0.03}_{-0.04}$

GRAVITATIONAL WAVE INTERFEROMETERS

Summary of Ligo-Virgo-KAGRA Binary mergers

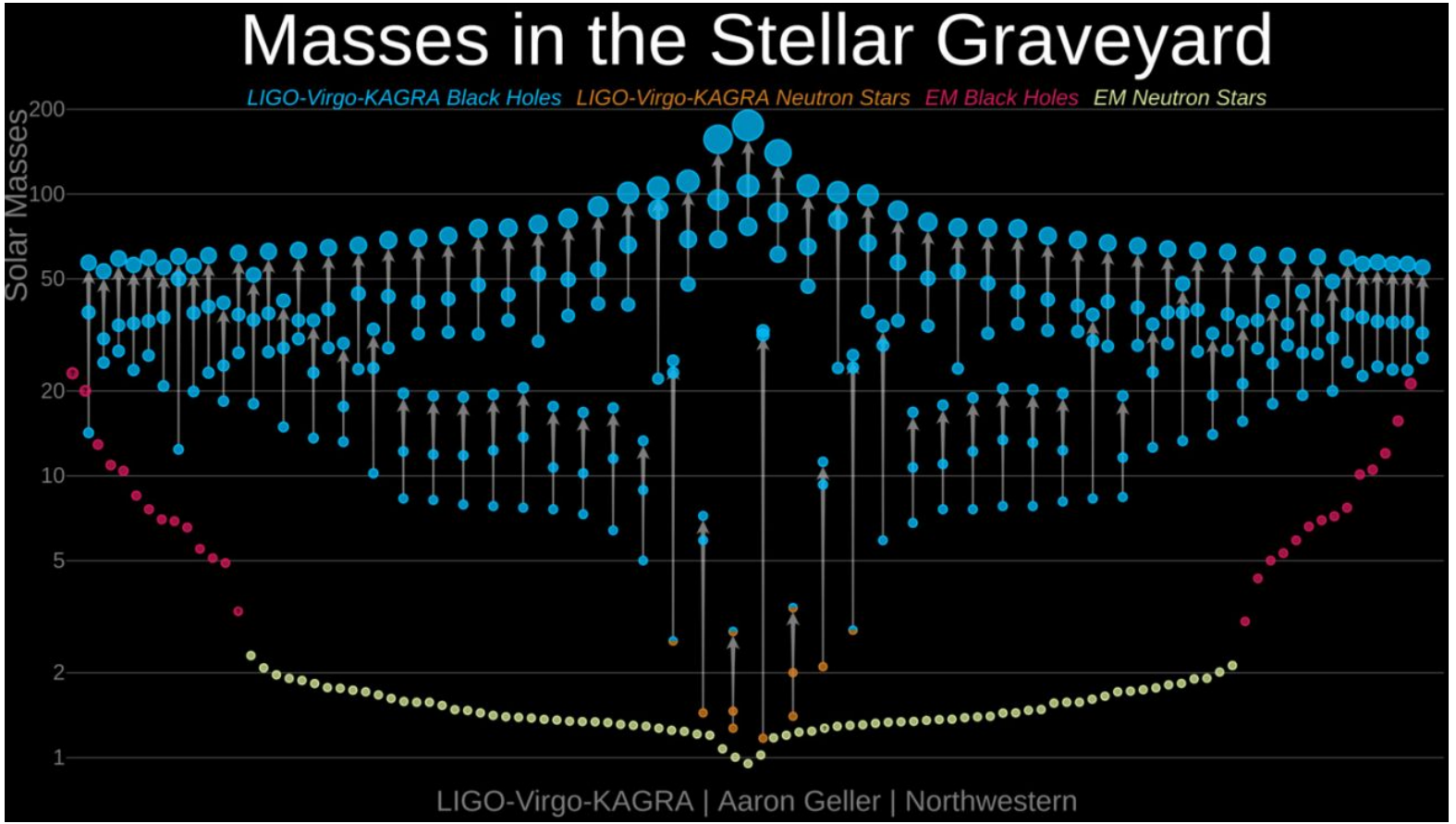

STANDARD SIRENS

GW 170817: First Binary Neutron star merger

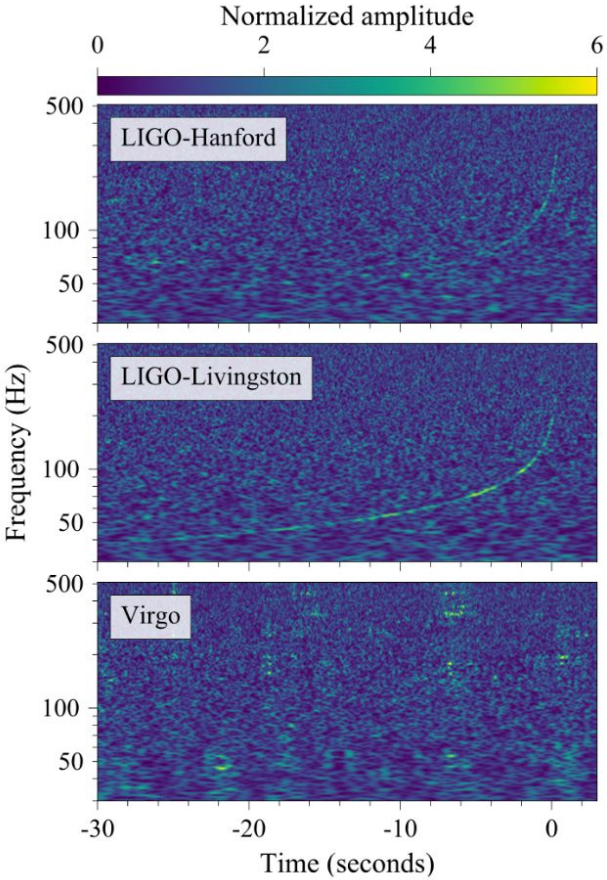

Triangulation of the GW signal:

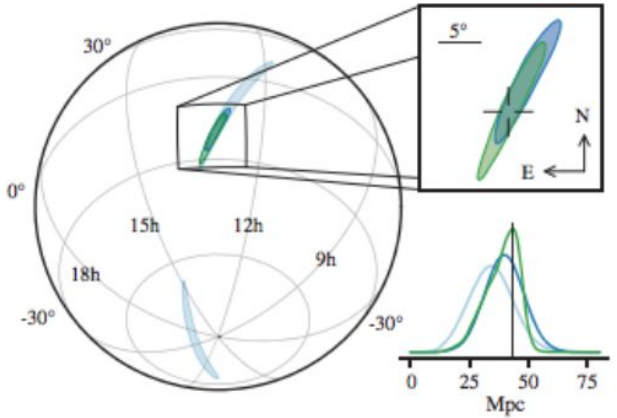

FIG. 3. Sky location reconstructed for GW170817 by a rapid localization algorithm from a Hanford-Livingston (190 deg^2, light blue contours) and Hanford-Livingston-Virgo (31 deg^2, dark blue contours) analysis. A higher latency Hanford-Livingston-Virgo analysis improved the localization (28 deg^2, green contours). In the top-right inset panel, the reticle marks the position of the apparent host galaxy NGC 4993. The bottom-right panel shows the *a posteriori* luminosity distance distribution from the three gravitational-wave localization analyses. The distance of NGC 4993, assuming the redshift from the NASA/IPAC Extragalactic Database [89] and standard cosmological parameters [90], is shown with a vertical line.

STANDARD SIRENS

Multi-wavelength follow-up:

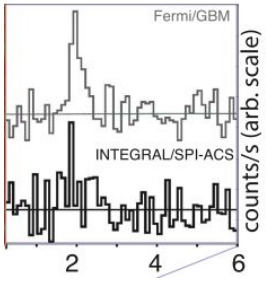

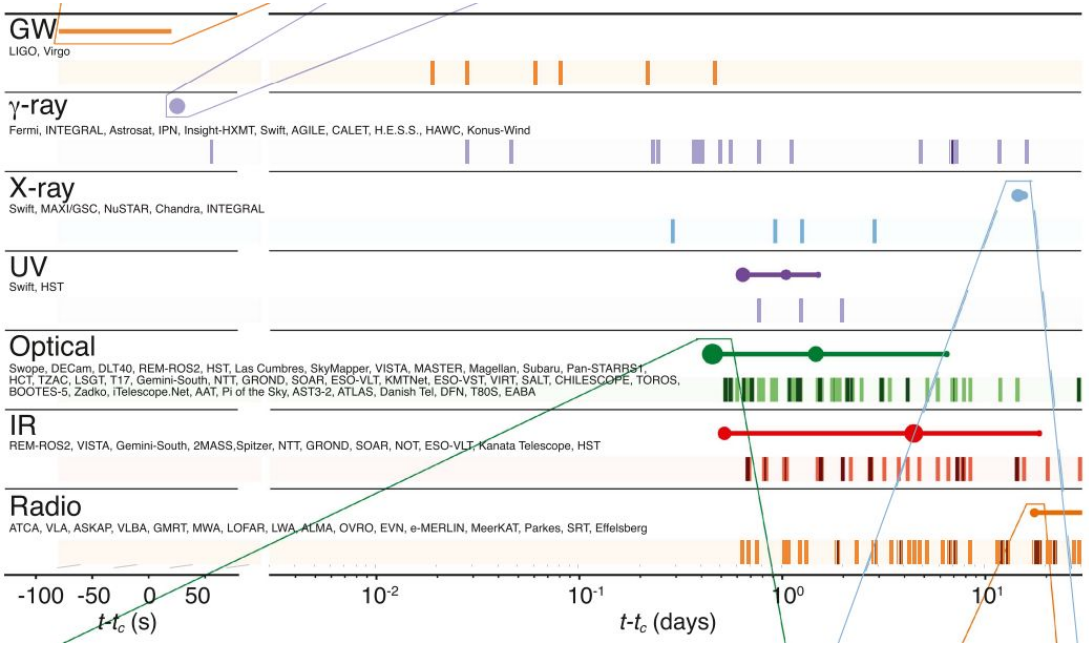

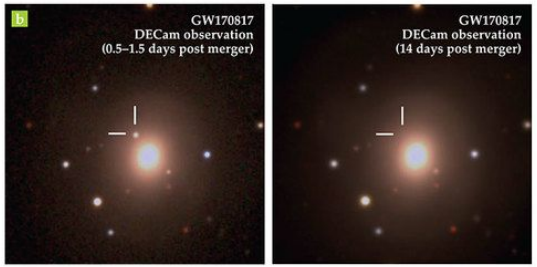

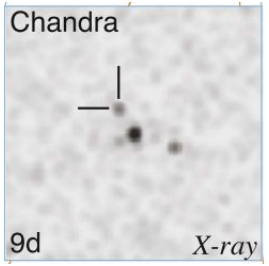

STANDARD SIRENS

- GW are “self-calibrating” sources (Schutz 1986)

$$h \sim D_L^{-1}$$

  - Direct measurement of luminosity distance
  - “Standard sirens”
- In general, no redshift from GWs (Krolak & Schutz 1987)

$$m_{obs} = m_{src}(1+z)$$

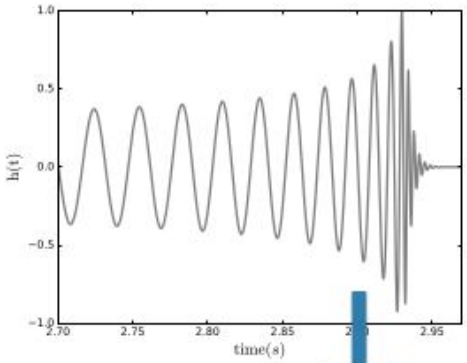

D_L

z

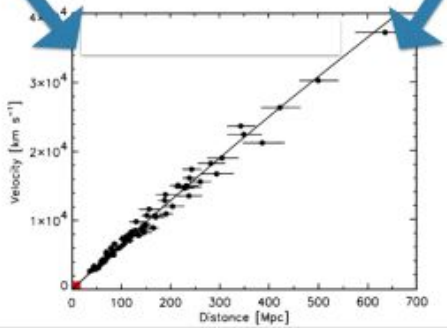

STANDARD SIRENS

- From GW alone

$$D_L = 44^{+3}_{-7}\,\mathrm{Mpc}$$

- NGC 4993

$$z = 0.0098$$

$$H_0 = 70^{+12}_{-8}\,\mathrm{km\,s^{-1}\,Mpc^{-1}}$$

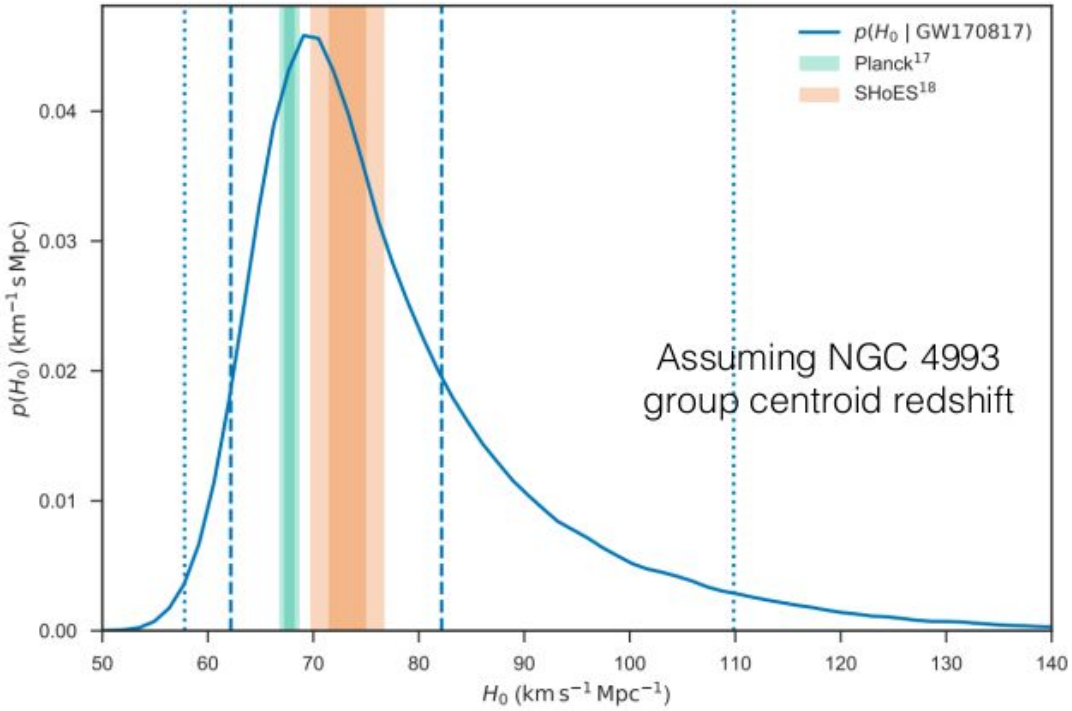

arxiv:1710.05835

DARK STANDARD SIRENS

A dark siren is a gravitational wave event without EM counterpart. Most binary mergers, and in particular binary black hole (BBH) mergers, do not have associated electromagnetic counterparts. However, in the absence of such a counterpart signposting the host galaxy directly, we can still use the gravitational-wave observations to give us information about the sky position of the source – and in this way narrow down the host galaxy to a set of candidate galaxies in this region. Combining redshift information from all of these possible host galaxies then allows us to measure H_0 statistically.

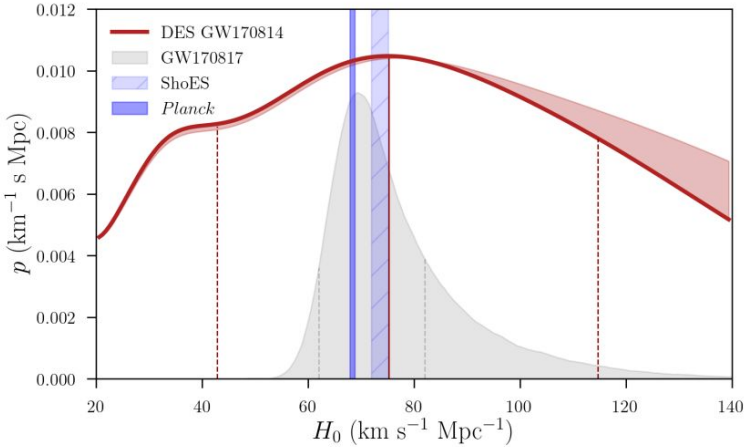

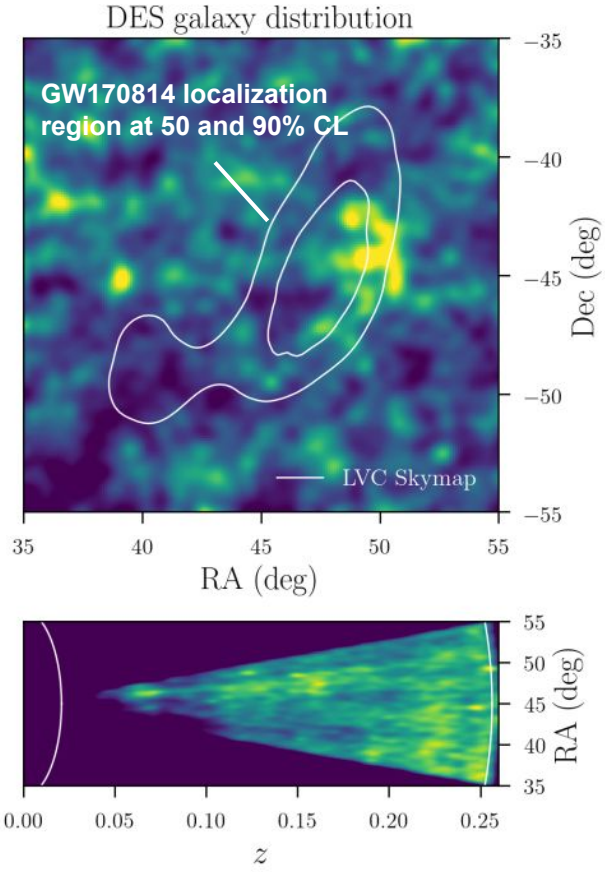

https://arxiv.org/pdf/1901.01540

GRAVITATIONAL WAVE BACKGROUND

Cosmological GW background: signature of the Early Universe Inflation, preheating, reheating (10^{-18} – 10^{8} Hz) Phase transitions (a narrow band feature peaking at 10^{-12} Hz + broadband component in the band 10^{-5} – 1 Hz). Cosmic strings (10^{-10} – 10^{10} Hz); Alternative cosmologies

Astrophysical GW background: Such a GW background may result from the superposition of a large number of unresolved sources since the beginning of stellar activity. Its detection would constrain the physics of compact objects, the IMF, the star formation history. It would probe the Universe at z ~ 0.02–10. However, from the point of view of detecting the cosmological background produced in the primordial Universe, the astrophysical background is a 'noise', which could possibly mask the relic cosmological signal

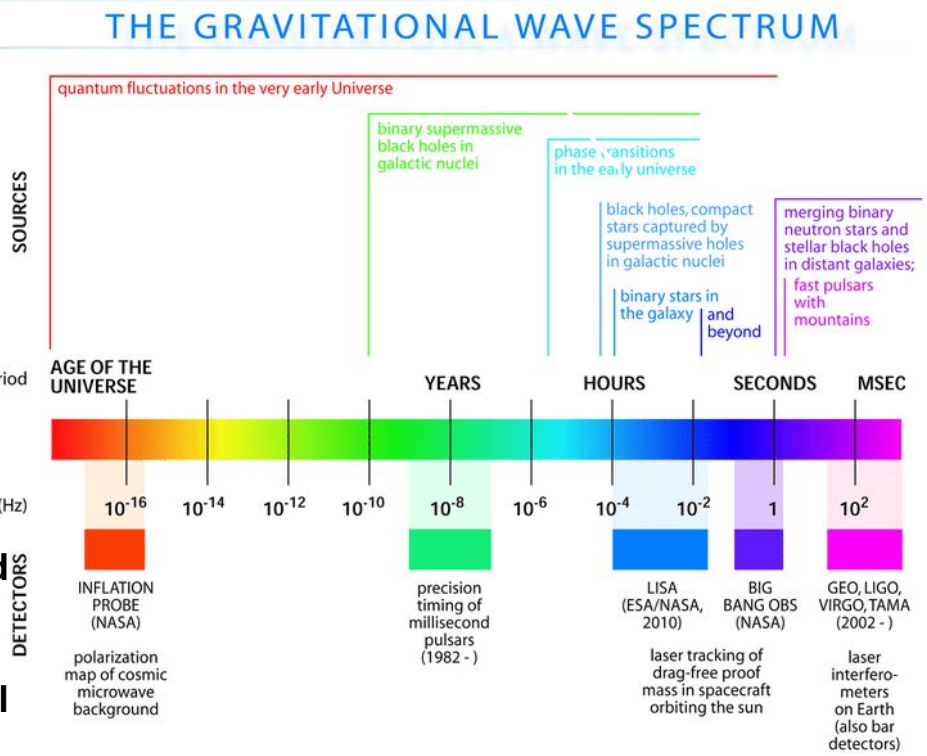

PULSAR TIMING ARRAY

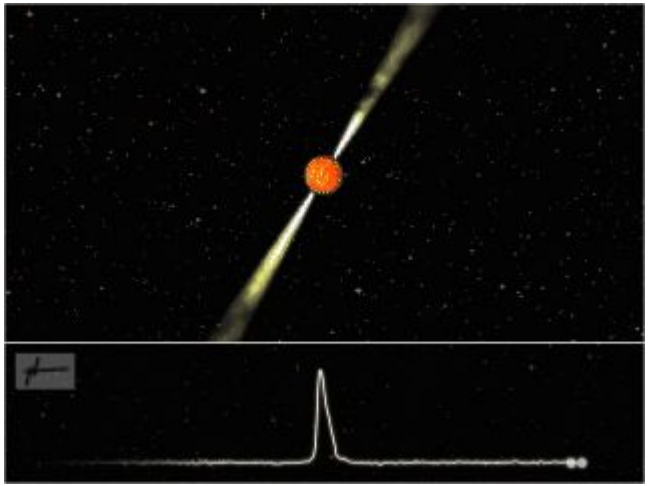

Highly magnetized rotating neutron stars, ultra-precise stellar clocks:

- **Beamed radio pulses emitted from magnetic poles**
- **Periods of 10^{-3}-1 s.**

Array of pulsars across the Milky Way can be used GW detector of galactic dimensions:

- **Look for tiny distortions in pulse travel times caused by nanohertz GWs.**
- **Signal builds up over time; monitor PTA over years and decades.**

Which pulsars are suitable ?

Ordinary pulsars:
~ 3350 known objects;
NS_{age} < few 10^7 yr

relatively long pulses & rotational irregularities

Recycled pulsars:
~ 500 known objects;
NS_{age} > 10^8-10^9 yr

The most rapidly rotating are known as millisecond pulsars

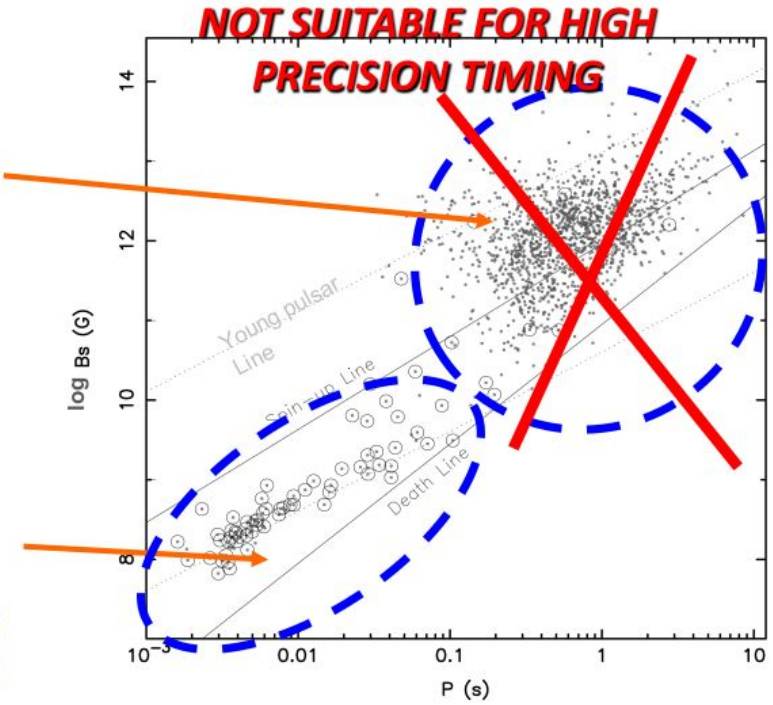

ATNF Pulsar Catalogue Feb 2024

Pulsar periods can sometimes be measured with unrivalled precision E.g. on Jan 16, 1999, PSR J0437-4715 had a period of:

5.757451831072007 ± 0.000000000000008 ms

PULSAR TIMING ARRAY

- **Clock errors**
  All pulsars have the same TOA variations:
  Monopole signature
- **Solar-System ephemeris errors**
  Dipole signature
- **Gravitational waves background**
  Quadrupole signature

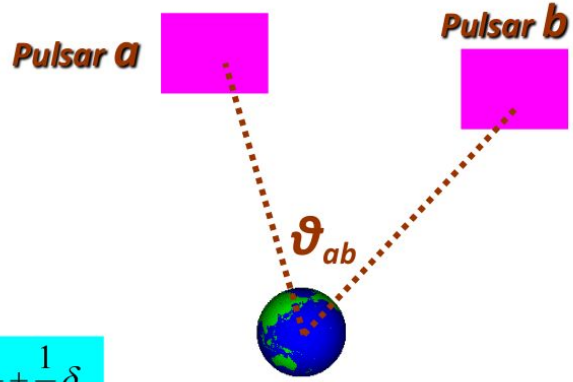

$$\zeta(\theta_{ab}) = \frac{3}{2}\left(\frac{1-\cos\vartheta_{ab}}{2}\right)\log\left(\frac{1-\cos\vartheta_{ab}}{2}\right) - \frac{1}{4}\left(\frac{1-\cos\vartheta_{ab}}{2}\right) + \frac{1}{2} + \frac{1}{2}\delta_{ab}$$

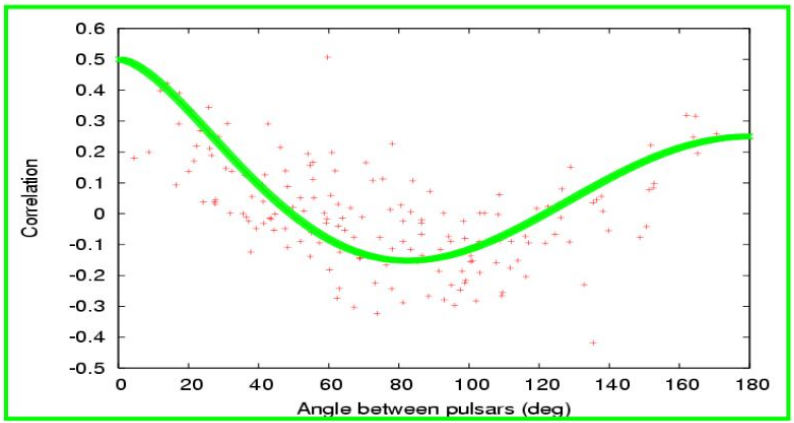

Hellings & Downs [1983]:
correlation that an isotropic, stationary and stochastic GWB leaves on the timing residuals of pairs of pulsars *a* and *b* separated by angle ϑ_{ab} in sky

[slide adapted from Manchester 11]

PULSAR TIMING ARRAY

PULSAR TIMING ARRAY

Evidence (2 - 4.6 σ) for quadrupole correlation signal from different collaborations.

The signal can be interpreted as:

- Cosmic population of in-spiralling SMBHB (realistic)
- New Physics (speculative)

2306.16213: NANOGrav

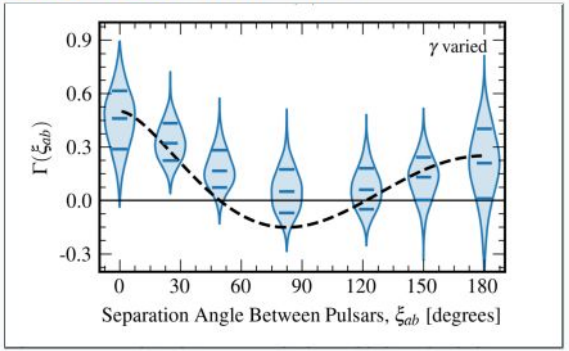

68 pulsars, 16 yr of data, HD at $\sim 3 \cdots 4\,\sigma$

2306.16214: EPTA+InPTA

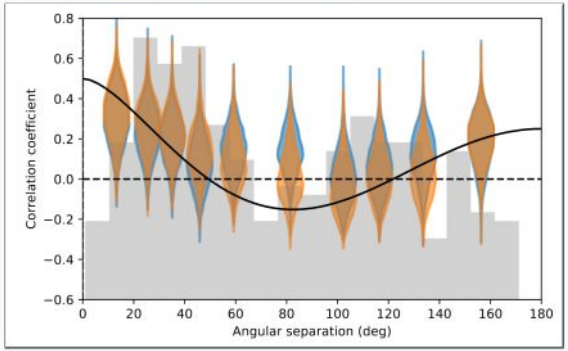

25 pulsars, 25 yr of data, HD at $\sim 3\,\sigma$

2306.16215: PPTA

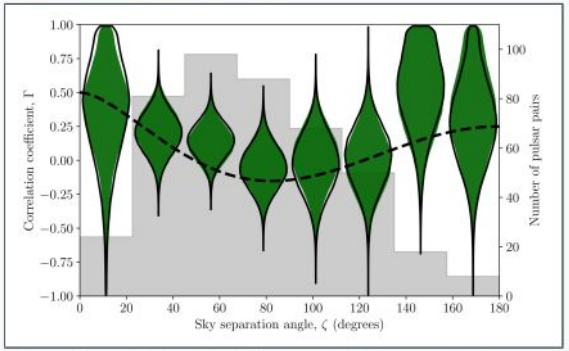

32 pulsars, 18 yr of data, HD at $\sim 2\,\sigma$

2306.16216: CPTA

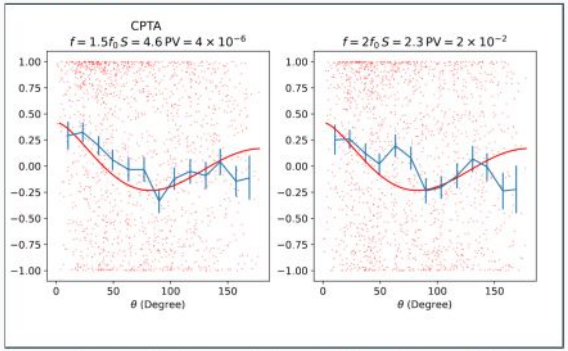

57 pulsars, 3.5 yr of data, HD at $\sim 4.6\,\sigma$

GW background due to Super Massive Black-Hole Binaries (SMBHBs):

It's well known that current paradigm is that [e.g. Ferrarese & Merrit 2000]

- mergers are an essential part in galaxy formation and evolution
- nuclei of most (all?) large galaxies host Massive BH(s) i.e. mass $M \gtrsim 10^6\ M_\odot$

When reaching orbital separation a of less than about 1 pc, GW emission at frequency f become the dominant term in energy loss, making the MBH binary to shrink faster and faster

$$f \sim 3\ \text{nHz} \left[\frac{M}{10^9\ M_\odot}\right]^{1/2} \left[\frac{a}{0{,}01\ \text{pc}}\right]^{-3/2}$$

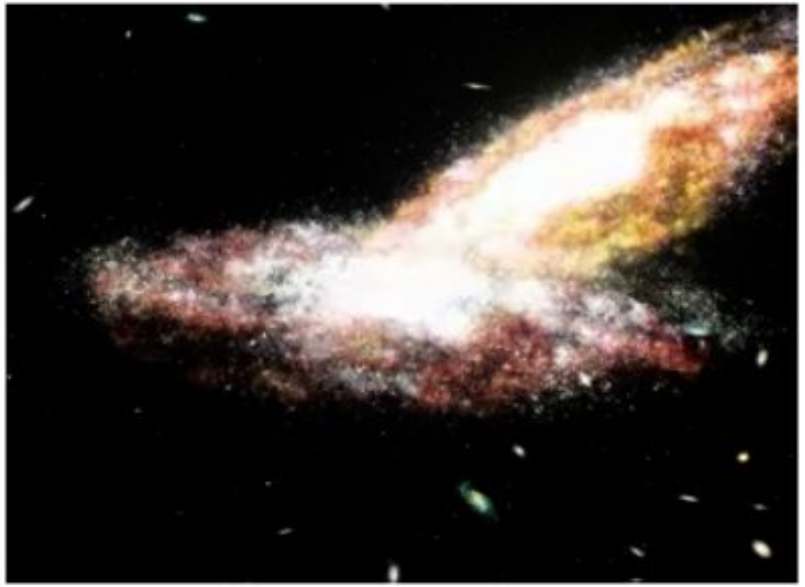

[© CSIRO]

Expected Strain Spectrum of GWB:

In the simplest picture, the expected amplitude spectrum from the ensemble of these MBH binaries (supposed to be isotropic and stochastic) is [e.g. Phinney 2001; Jaffe & Backer 2003]

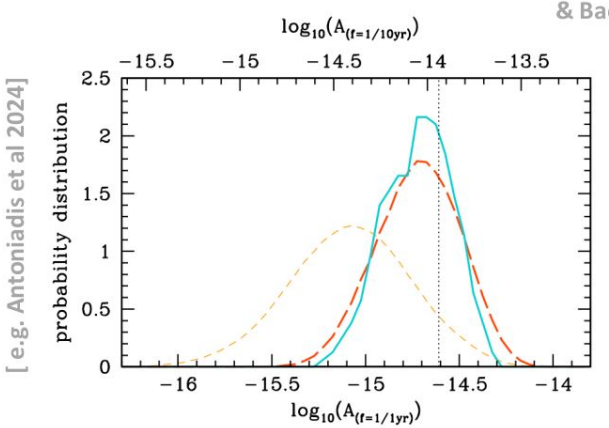

[e.g. Antoniadis et al 2024]

$$h_c(f) \sim f^{-\alpha} \quad \text{with} \quad \alpha = 2/3$$

with a "strain" amplitude h_c theoretically expected in a large range

[e.g. Jaffe & Backer 2003, Rosado et al 2015, Sesana et al 2016, Kelly et al 2017, Zhu et al 2019]

$h_c \approx 6 \bullet 10^{-17} \rightarrow 8 \bullet 10^{-15}$

around frequency $f_{GWB} = 1\ \text{yr}^{-1}$

$$P_{GWB}(f) \sim f^{-2\alpha-3} = f^{-13/3} \quad \text{for} \quad \alpha = 2/3$$

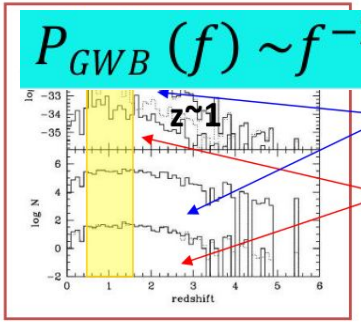

[Sesana,Vecchio et al

Max contribution from BH binaries at $z \approx 1$

Observed Strain Spectrum of GWB:

2306.16213: NANOGrav

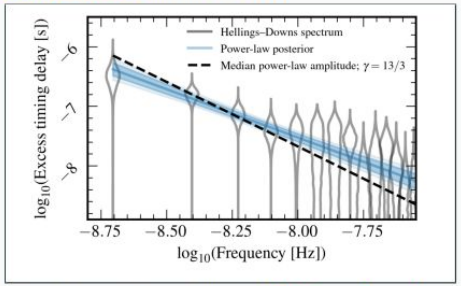

68 pulsars, 16 yr of data, HD at $\sim 3 \cdots 4\,\sigma$

2306.16214: EPTA+InPTA

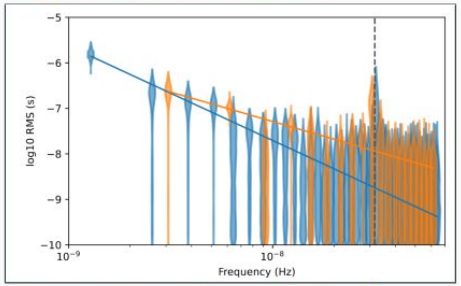

25 pulsars, 25 yr of data, HD at $\sim 3\,\sigma$

2306.16215: PPTA

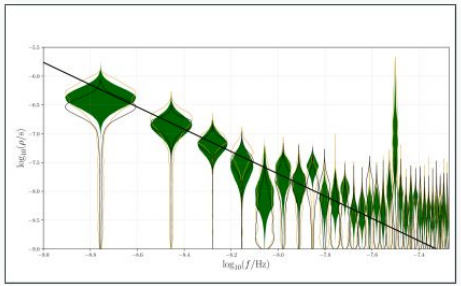

32 pulsars, 18 yr of data, HD at $\sim 2\,\sigma$

2306.16216: CPTA

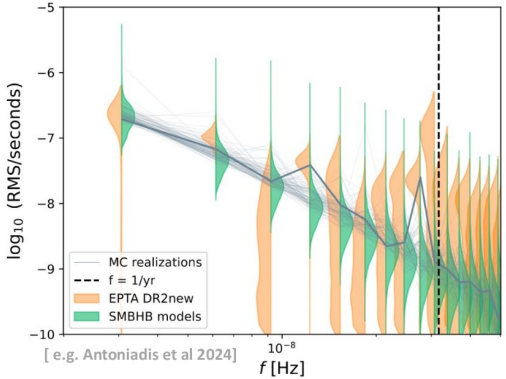

[e.g. Antoniadis et al 2024]

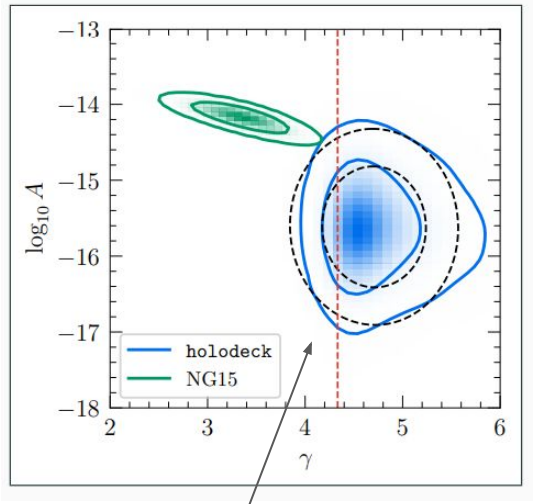

Simplest models of binary evolution (holodeck) struggle to explain the data (NG15), but many sources of systematic can hamper the interpretation of the results

Many Beyond-Standard-Model models predict GWB from the Big Bang:

Inflation

- Nonminimal blue-tilted models
- Interplay with CMB observables

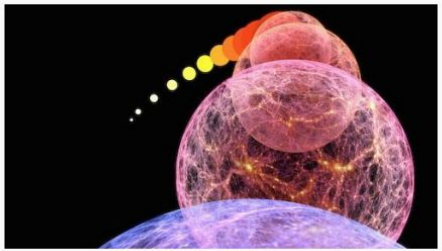

Phase transition

- Modified QCD transition, dark sector
- Complementary to laboratory searches

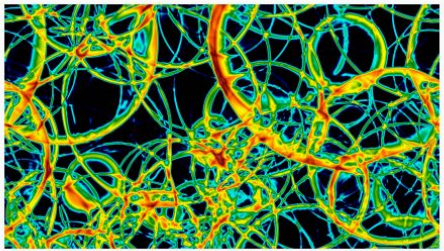

Cosmic defects

- Cosmic strings, domain walls
- Access to grand unified theories

Scalar perturbations

- Associated with primordial black holes
- PBH dark matter, supermassive BHs